Territorial risks

SIRMA

STRENGTHENING INFRASTRUCTURE RISK MANAGEMENT IN THE ATLANTIC AREA

Sensor selection & deployment guidelines

December 2022 (V1.0)

PUBLIC

SIRMA

STRENGTHENING THE TERRITORY'S RESILIENCE TO RISKS OF NATURAL, CLIMATE AND HUMAN ORIGIN

Application Code: EAPA_826/2018

Sensor selection & deployment guidelines

WP 5 WP Title Instrumenting Transportation Infrastructures for Extreme Natural Hazards

Deliverable ID	**D5.3**
Deliverable name	**Sensor Selection and Deployment Guidelines**
Lead partner	**UCD**
Contributors	UCD, Irish Rail

PUBLIC

SIRMA Project Synopsis

SIRMA

Territorial risks

SIRMA aims to develop, validate and implement a robust framework for the efficient management and mitigation of natural hazards in terrestrial transportation modes at the Atlantic Area, which consider both road and railway infrastructure networks (multi-modal). SIRMA leads to significantly improved resilience of transportation infrastructures by developing a holistic toolset with transversal application to anticipate and mitigate the effects of extreme natural events and strong corrosion processes, including climate change-related impacts. These tools will be deployed for critical hazards that are affecting the main Atlantic corridors that is largely covered by SIRMA consortium presence and knowledge. SIRMA's objectives will address and strengthen the resilience of transportation infrastructures by:

- Developing a systematic methodology for risk-based prevention and management (procedures for inspection, diagnosis and assessment);
- Implementing a decision-making algorithm for a better risk management;
- Creating a hierarchical database (inventory data, performance predictive models, condition state indicators and decision-making tools), where information can be exchangeable between entities and across regions/countries;
- Developing a real-time process for monitoring the condition state of transportation infrastructure;
- Enhancing the interoperability of information systems in the Atlantic Area, by taking account of data normalization and specificity of each country.

Territorial risks

Document Information

Document Name	Sensor Selection and Deployment Guidelines	
Version No.	V1.0	
Due date	31/12/2022	
Report date	29/12/2022	
Number of pages	40	
Lead Author	Vikram Pakrashi (UCD)	
Other Authors	Eugene OBrien, UCD Cathal Bowe, Irish Rail E. Alexandra Micu, UCD Claire McGeown, UCD Muhammad Arslan Khan, UCD David Hester, QUB	
Dissemination level	[Confidential]	

Document History

Ver.	Date	Description	Authors	Checked by
0.1	21/09/2022	Creation of the document		
1.0	29/12/2022	Completion of Document	Vikram Pakrashi, Cathal Bowe, E. Alexandra Micu, Eugen OBrien Claire McGeown Muhammad Arslan Khan David Hester	Eugen OBrien

Document Approval

Ver.	Name	Position in project	Beneficiary	Date	Visa
1.0					

Executive Summary

This report outlines sensor selection and deployment guidelines based on examples and experiences in the SIRMA project. A focus is kept around the topic of using the train bridge interaction for detecting features of interest, including damage. The report first considers the use of rotation as a possible feature for measurement and calibration for damage detection. Subsequently, the report looks into the idea of re-deployable sensors. Next, an IoT solution around instrumentation and measurement is presented. Finally, the use of train-bridge interaction as deployed in Irish Rail infrastructure, and in conjunction with the implementation of WP7 is discussed.

Table of Contents

1. Introduction

Measurement and monitoring strategies are particularly important for monitoring out railway infrastructure networks and related other infrastructure as well. This is not just for detecting damage but also for other features of interest like efficacy of repair and presence of trains. With time, extensive improvement of technology and monitoring has been made but challenges still remain, especially via the paucity of examples and benchmarks for good guidance for sensor selection and deployment.

This report provides some of these examples through the SIRMA project. A number of examples of sensors and their placements are discussed, as are instrumentation and measurement strategies. Implementation via WP7 with Irish Rail is also discussed and the use in real-sites are highlighted.

The performance of measurement and details are presented and it creates a context around detection. These not only link with WP7, but also provide context and connection to WP4. Over time and with a range of such implementations, better understanding and a conduit towards standardisation (e.g D3.2, WP3) can be achieved.

At this point, sensors, instrumentation and measurement are moving fast in terms of innovation and there are often inadequate examples to assess their performance under realistic situations. This report provides some of these estimates and creates realistic targets for better interpretation of results. It also ensures that the expectations of various markers of detection are not overpromised and the boundaries of estimates and accuracy are well established.

Figure 1: Example of an embedded vibrating wire strain gauge for monitoring repair of an impact damaged prestressed bridge in Ireland.

2. Rotation Measurement as an Important Marker for Monitoring

2.1 Context

The measurement of rotation has been investigated in SIRMA in detail and was found to be representative of damage and other features of interest. There are signatures of these features of interest in the data and appropriate measurement and monitoring can obtain relevant information on them. Data from real bridges were considered in this regard as were laboratory experiments. Of particular note is the fact that rotation measurement devices are often very expensive and require changes to be made to instrumentation, but the methods presented consider standard accelerometers and strain gauges and thus are better suited to extend existing instrumentation.

2.2 Monitoring Narrow Bridges using Rotation via Weigh-in-Motion Systems

Conventional strain-based B-WIM system data is combined with the damage sensitive rotation-based B-WIM system data for health monitoring. When a bridge experiences a localised loss of stiffness due to damage, rotation sensors respond with increased support rotations under vehicular loading. As the B-WIM system will have been calibrated for the healthy bridge, the GVWs will be overestimated, providing a statistical indicator of damage. Provided it is a narrow bridge (no significant change in load sharing transversely), the strain-based B-WIM system will continue to weigh passing vehicles accurately, providing reference values for their weights. Thus, any divergence in the vehicle weights inferred by the two systems, is an indicator of bridge damage. A strength of this approach is that there is no need to compare the new data to healthy bridge baseline data, reducing complications such as data management issues and difficulty in controlling the effects of varying environmental conditions. A further advantage of this approach is the ability to combine the measured responses to a large population of vehicles, which has the potential to amplify the effects of low damage levels.

Inclinometers, or tiltmeters, measure rotation relative to an ‘artificial horizon’. Thie accuracy and performance have significantly improved, and it is now possible to measure inclinations to microradian (10^{-6} rad) accuracy. Here we used Honeywell QA-750 accelerometers which can detect frequencies very close to 0 Hz (i.e. gravity), making it possible to convert the output signal into rotation. The relationship between the static (gravity) component of the accelerometer reading and the angle of rotation is illustrated in Figure 2. When the accelerometer is horizontal and stationary, it records zero. When the accelerometer is in a verticle orientation it records 9.81 m/s2 (or 1 g), and when in the upwards position it records -9.81 m/s2 (or -1 g). When the accelerometer is attached longitudinally to a beam and the beam starts to rotate, as illustrated in Figure 3, the angle of rotation, Θ, is:

$$a = g \sin \Theta \quad (1)$$

where a = accelerometer reading, g = acceleration due to gravity (i.e. 9.81 m/s2), Θ = angle of rotation. It follows that:

$$\Theta = \sin^{-1}(a/g) \tag{2}$$

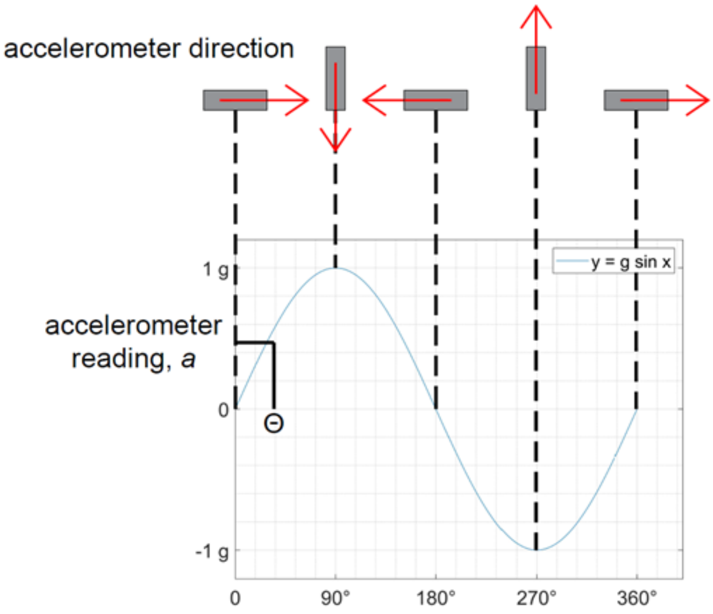

Figure 2: Calculating rotation from an accelerometer: Response of a stationary accelerometer to its angle of orientation, Θ; (b) Accelerometer attached to a bridge

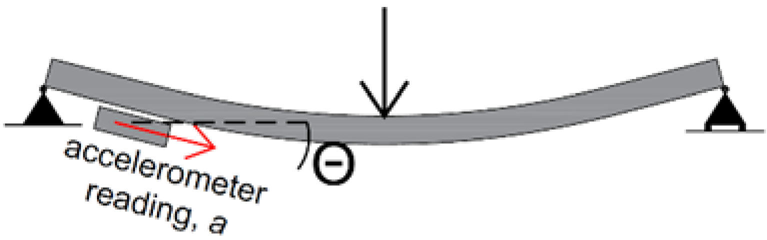

Figure 3: Calculating rotation from an accelerometer: Accelerometer attached to a bridge

Data from a test on a bascule bridge (Figure 4) was used where it behaves as a simply supported structure with a span of 17.8 m. During the test, the bridge was loaded with a 4-axle 32 tonne truck. The rotation at the two supports, shown as points A and B in Figure 4, was measured using accelerometers orientated in the longitudinal direction. Figure 5 shows the measured peak rotation to be approximately 0.1 degree.

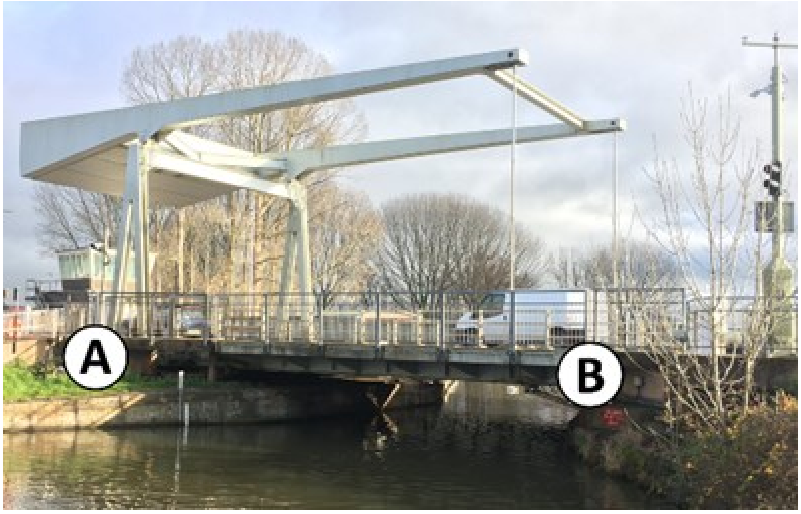

Figure 4. Rotations recorded on a bascule bridge: Elevation of the test structure and locations on measurement;

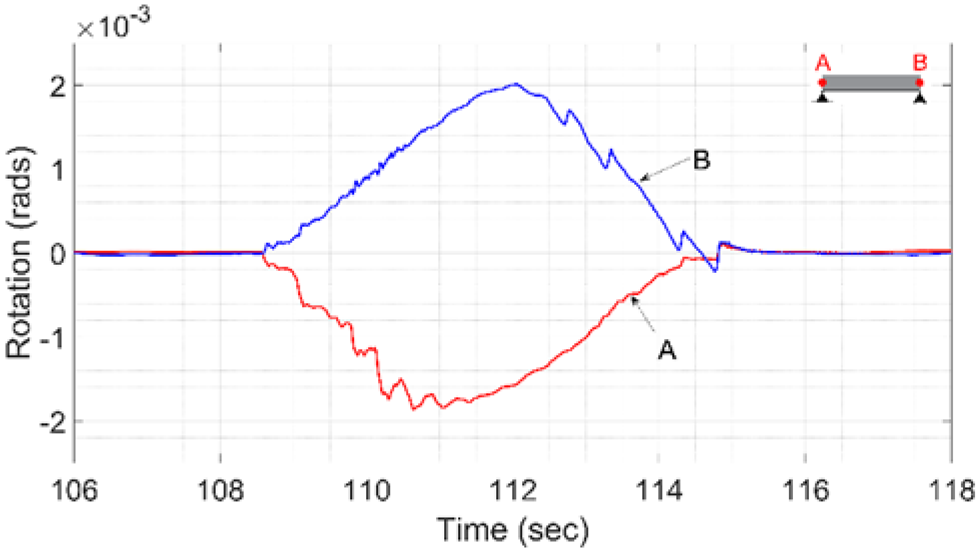

Figure 5. Rotations recorded on a bascule bridge: Rotation time history at supports

The influence line for strain or rotation at a point, is estimated and since the beam is narrow and determinate, bending moment is not affected by the flexural rigidity. As a result, the strain is only affected by the section properties at the sensor location.

This is why the influence line for strain is unaffected by damage far away from damage but is affected close to it. It is difficult to have a dense sensor network to capture such changes and so methods must be made for sparse deployment of sensors.

Rotation at any point is affected by the flexural rigidity in all segments of the beam and is sensitive to damage anywhere. The largest rotation responses (and therefore those with the best signal-to-noise ratio) are for the sensors at the beam supports and it can be used for detecting damage well. Figure 6 presents an experimental validation of such sensor deployment.

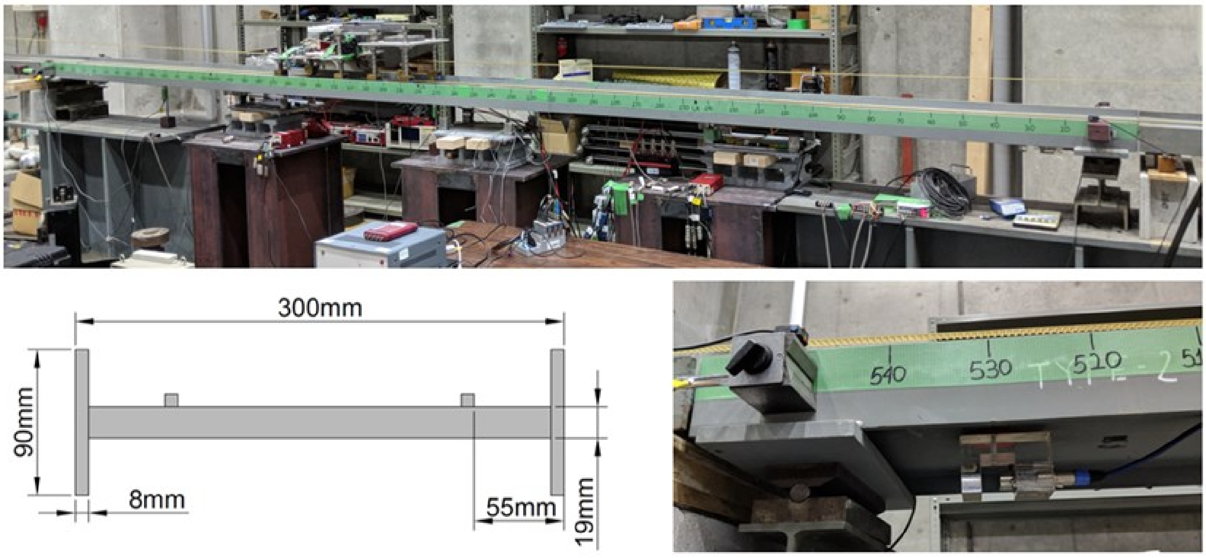

Figure 6. Test structure elevational view, cross-section dimensions, roller end support and accelerometer.

Table 1 shows the details of beam. The vehicle used is a 4-axle tractor-trailer shown in Figure 7 with the axle weights and spacings listed in Table 2. It crosses the beam at a constant speed controlled by an electronic pulley system, with acceleration and deceleration spans on either side of the beam. Laser axle detectors, placed at the start and end of the span, recorded the time of arrival and departure and hence the average speed.

Electrical resistance strain sensors installed at approximately one-quarter and three-quarter span and triaxial accelerometers measure rotation (the same as used in the bascule bridge). Rotation of the test structure is of similar magnitude to that of the previous bascule bridge. Data acquisition was done at a 2048 Hz sampling rate using an NI9237 data acquisition system, controlled by a computer.

Span length	5.4 m
Young's modulus	210 x10^9 N/m^2
Density	7.8 x10^3 kg/m^3
Area of section	7.04 x10^{-3} m^3
Second moment of area	1.136 x10^{-6} m^4

Table 1. Properties of scaled structure

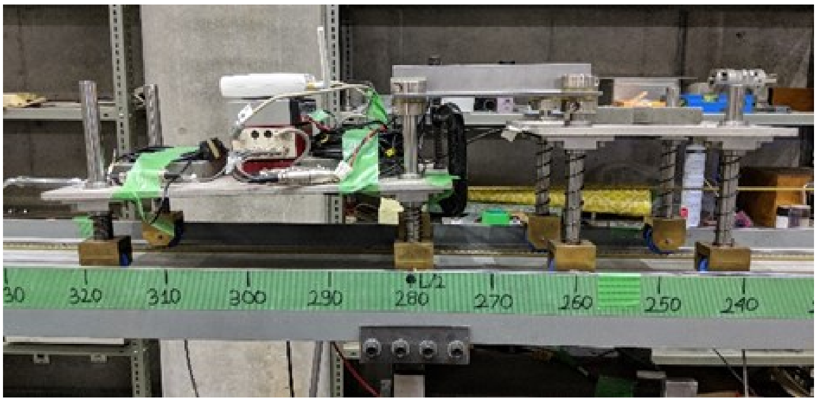

Figure 7. Example of model vehicle

Axle Number	Weight (kg)	Axle spacing (mm)
Axle 1	12.70	0
Axle 2	14.75	400
Axle 3	8.05	210
Axle 4	6.70	190

Table 2. Properties of model vehicle

Sensor locations are provided in Figure 8.

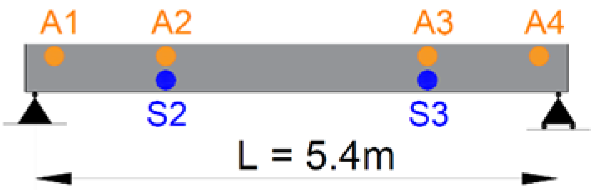

Figure 8. Sensor locations in test beam

The acceleometers are placed from the left as: A1: 0.2 m, A2: 1.44 m (≈L/4), A3: 4.14 m (≈3L/4), A4: 5.2 m while the strain gauges are placed from the left as S2: 1.44 m (≈L/4) and S3 4.14 m (≈3L/4). Since stiffness change represents damage, a 'negative damage' is considered by adding stiffness to the structure (Figure 9).

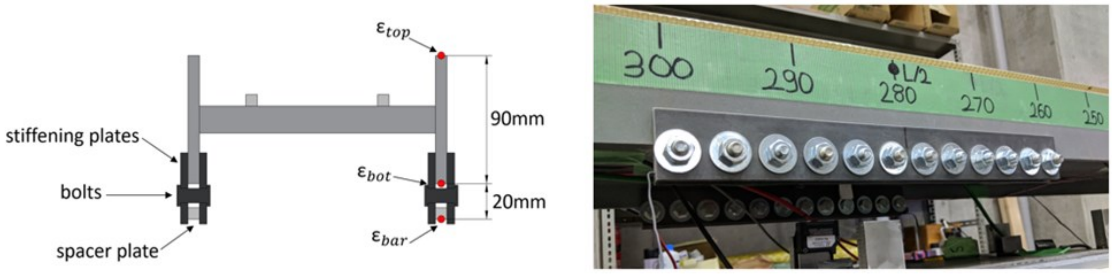

Figure 9. Stiffening plates attached to bridge. Cross-section showing additional strain gauges; Stiffening plates attached at midspan of test bridge.Sensor locations in test beam.

The gross vehicle weights estimated from a weigh in motion type approach demonstrates how such estimates are related to damages. Figure 10 demonstrates this.

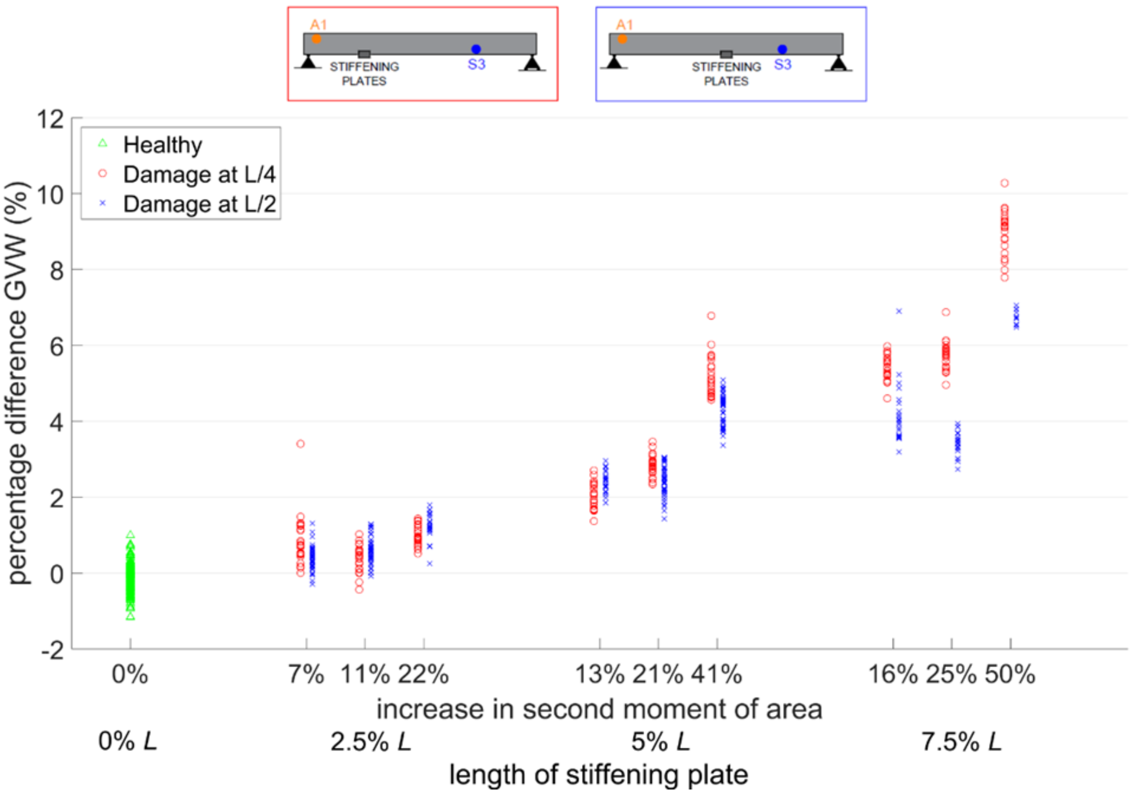

Figure 10. Percentage difference in gross vehicle weight inferred from one rotation and one strain sensor as a result of stiffening plates

See details in: Huseynov, F., Hester, D., Obrien, E. J., McGeown, C., Kim, C. W., Chang, K., & Pakrashi, V. (2022). Monitoring the Condition of Narrow Bridges Using Data from Rotation-Based and Strain-Based Bridge Weigh-in-Motion Systems. *Journal of Bridge Engineering*, *27*(7), 04022050.

2.3 Load Distribution Between Girders for Monitoring Bridges

The load distribution among beams in a 3-dimensional bridge model under normal traffic loading and the resulting effect of damage was investigated next represented as modelled as a localised loss of stiffness in a beam. The Vransko bridge in Slovenia was considered here (Figure 11) and modelled as Figure 12.

Figure 11. Elevation of Vransko bridge

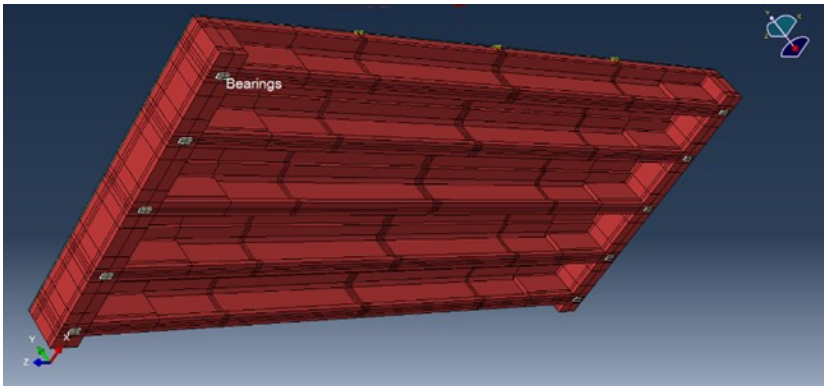

Figure 12. 3D Fintie Element Model of Vransko Bridge with damage as local loss of stiffness

Such model based damage assessments and esimtates of measurements can often be useful before implementing sensors.

The frequency of gross vehicle weights are provided in Figure 13 while Figure 14 shows how girder distribution can be used as a marker for monitoring through traditional strain measurements.

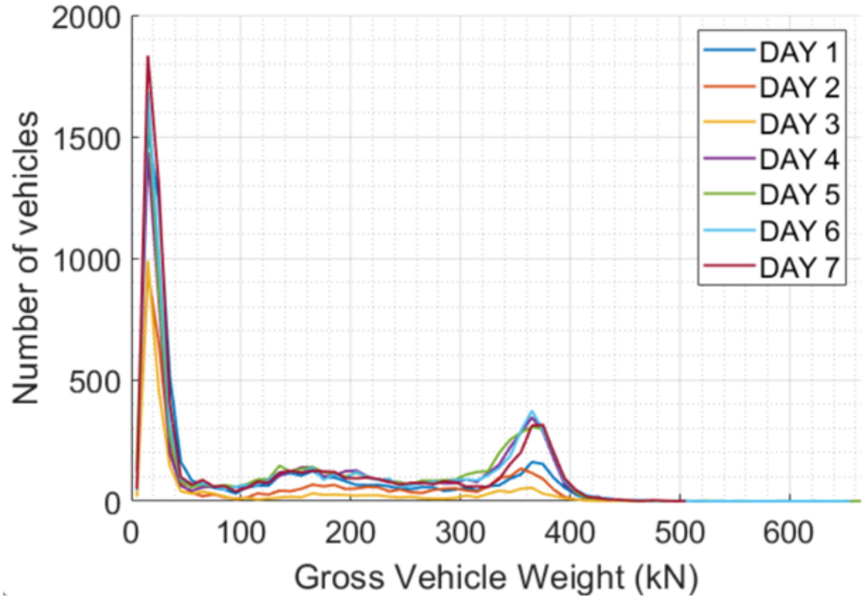

Figure 13. Gross Vehicle weights on Vransko Bridge

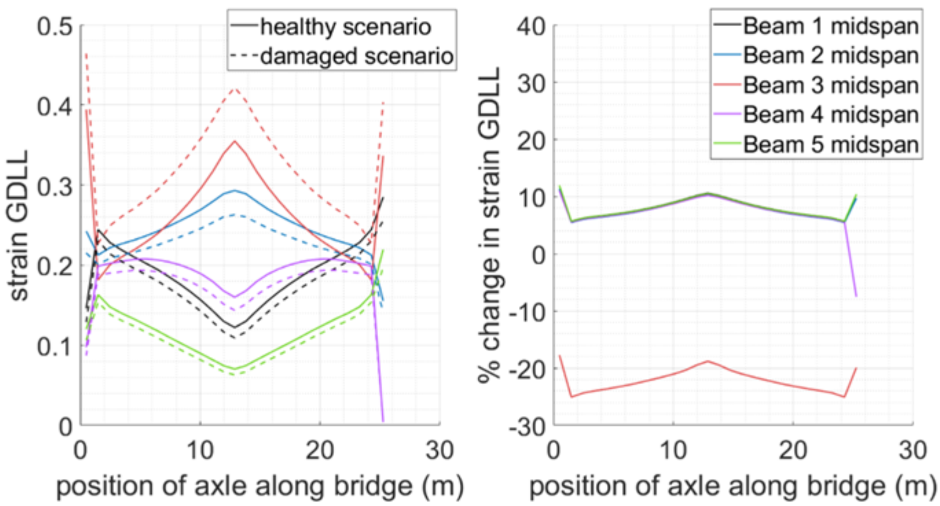

Figure 14. Change in strain via girder distribution of girder distribution longitudinal line (GDLL) of 3-dimensional finite element model due to a unit axle load with damage of 8% loss of stiffness at midspan of beam, including Strain GDLL along each beam and Percentage change in strain GDLL along each beam.

2.4 Using Vehicular Pitch for Monitoring Scour

The idea of instrumenting traversing vehicle on a bridge is exploited next and the pitch of the vehicle is considered for monitoring and detecting scour. An example of the instrumented vehicle is presented in Figure 15.

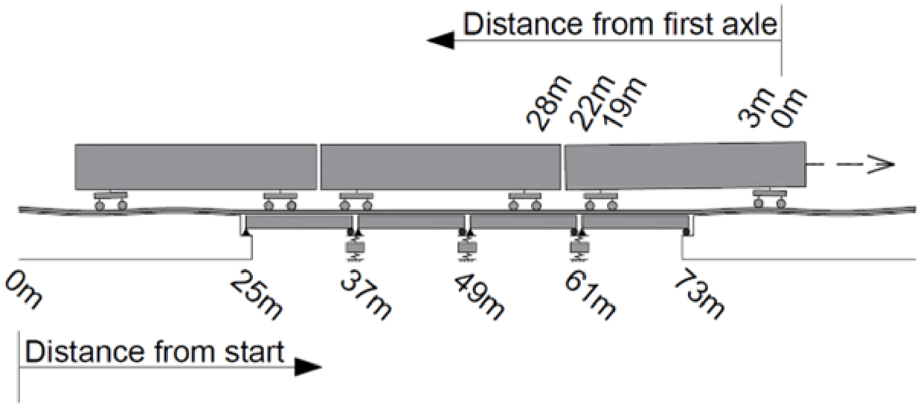

Figure 15. A schematic of an instrumented vehicle for scour monitoring through pitch.

The method of monitoring is presented in Figure 16. An example of using a carriage response for such detection is given in Figure 17.

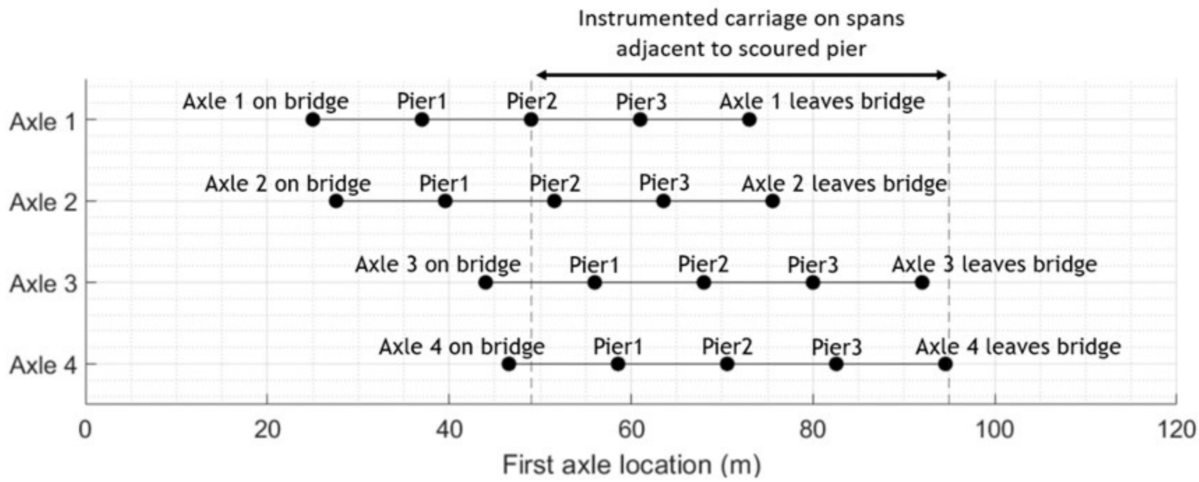

Figure 16.. An idea of measurement of vehicle based detection of damage in bridge (scour in this case)

Figure 18 shows a scaled experiment on this concept while Figure 19 shows the validation of the concept. This idea can be linked to traversing trains over bridges and such concepts will be taken up in the following sections of this report.

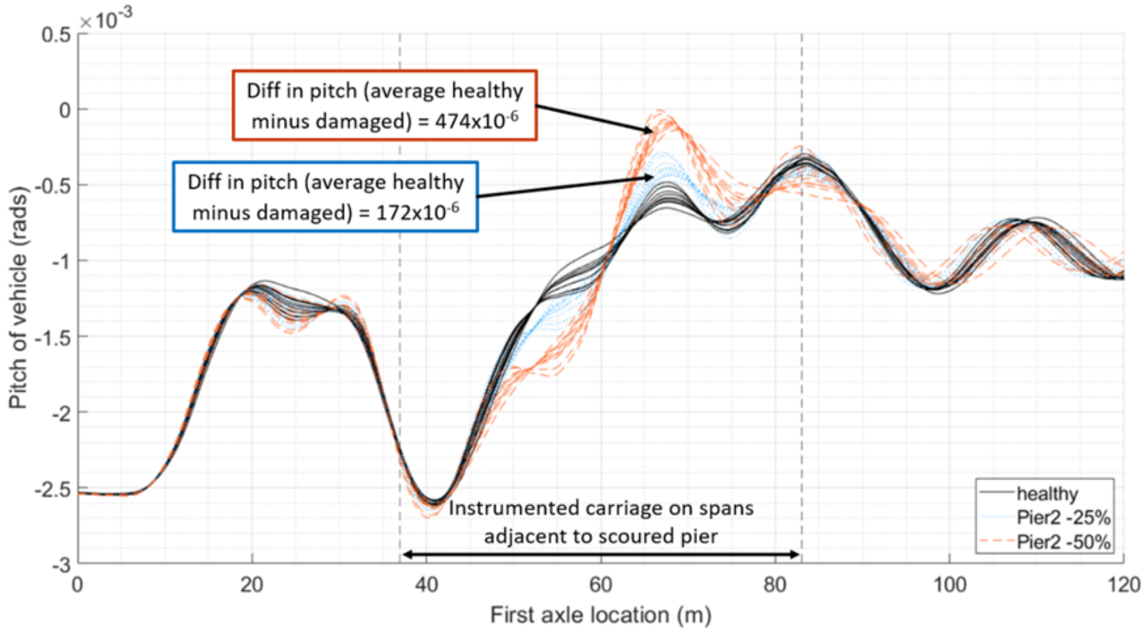

Figure 17. Difference in vehicle pitch as a damage indicator where the damage is loss of stiffness in pier

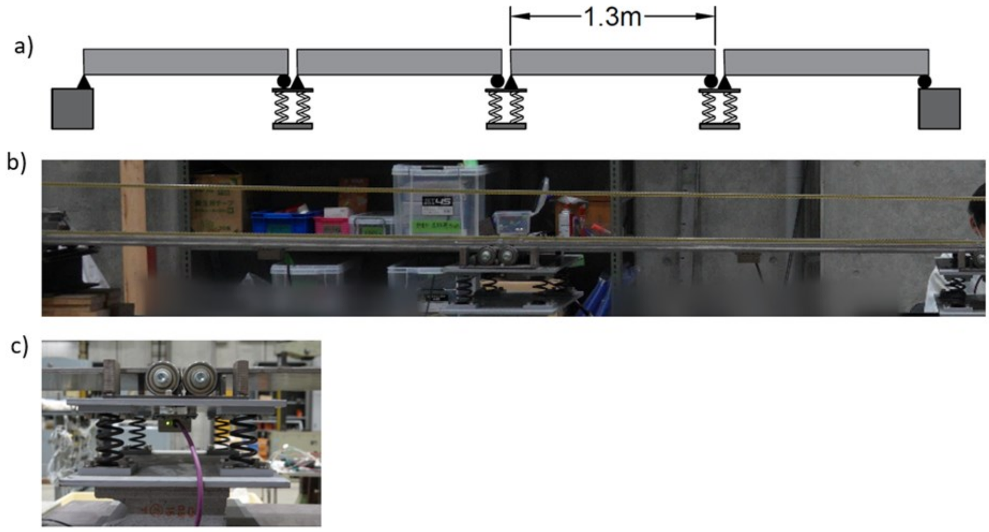

Figure 18. Experimental setup for scaled testing for detecting pier stiffness with pitch

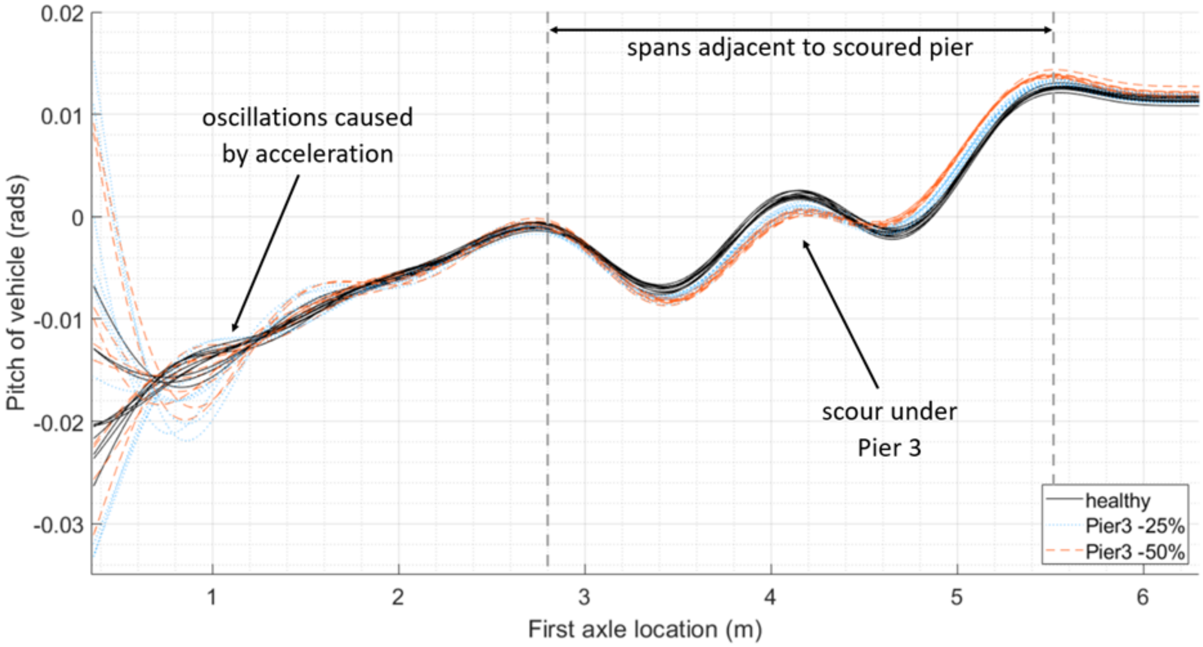

Figure 19. Experimental validation of pier stiffness loss from scour using vehicle pitch

3. Re-Deployable Sensors for Monitoring

3.1 Context

A method is proposed here where a small number of sensors are moved along the bridge and are re-deployed for various segments by changing the location of the sensors on the bridge with time and independently of traffic movement to obtain the modal parameters and the variations due to damage in the form of changes in rotational stiffness of the boundary condition of the bridge. This approach does not need indirect methods of analyses, which is typical for drive-by measurements using instrumented vehicles for which vehicle conditions are required to be known precisely and uncertainties are introduced in real life from lack of control over the vehicular characteristics and their movement. The proposed approach with re-deployable sensors allows a high-density array of measurement points to be monitored without using a large number of sensors.

3.2 Details of Rehabilitation

The proposed concept of using re-deployable sensors was validated through a full-scale study. The Oranmore bridge (UBG165) (Figure 20) in Co. Galway, Republic of Ireland was selected for this purpose. UBG165 has an 18.3m long single-span skewed steel deck and carries one operational rail track. The bridge consists of 2 primary longitudinal, 8 secondary transverse and 4 tertiary longitudinal steel beams with a thin steel plate deck. The bridge is 8.8m wide and is skewed at an angle of 48.5o.

Figure 20. Photograph of Oranmore Bridge used in this study

There was uncertainty about the support conditions (Figure 21) and the bridge was rehabilitated.

Figure 21. Support condition of Oranmore Bridge before rehabilitation

The ends of the deck were repaired and new bearings and abutments were installed (Figure 22). This is also an example of how UCD and Irish Rail combined their efforts and site-implementations in this regard.

Figure 22. Support condition of Oranmore Bridge after rehabilitation

Re-deployable accelerometers were used to assess the bridge before refurbishment on and then again after refurbishment. The field test data utilised bridge accelerations induced by passing trains and the first bridge mode shape was estimated before and after the replacement of support bearings.

Before the rehabilitation, the Oranmore bridge was inspected by the Irish operator and identified as being affected by inadequate bridge support conditions. Two primary, two secondary and two tertiary beams were resting on stone abutments at both sides of the bridge with unknown restraints to rotational capacity of the beams. Following refurbishment, the constraints at the boundaries were released and the field-implementation aimed to see if damage resulting in non-zero support stiffness could be identified following refurbishment.

3.3 Instrumentation and Measurement

Two triaxial wireless MEMS accelerometers (LORD MicroStrain G-Link-LXRS) were used to record the deck accelerations due to passing trains before and after the rehabilitation. In order to maintain time-synchronisation in-built beacon-based time-synchronisation tool is used, which is facilitated by a gateway, that communicates wirelessly to all the sensors before measuring the bridge accelerations in each stage. Six measurement locations were selected on the primary beam on the North side (Figure 23).

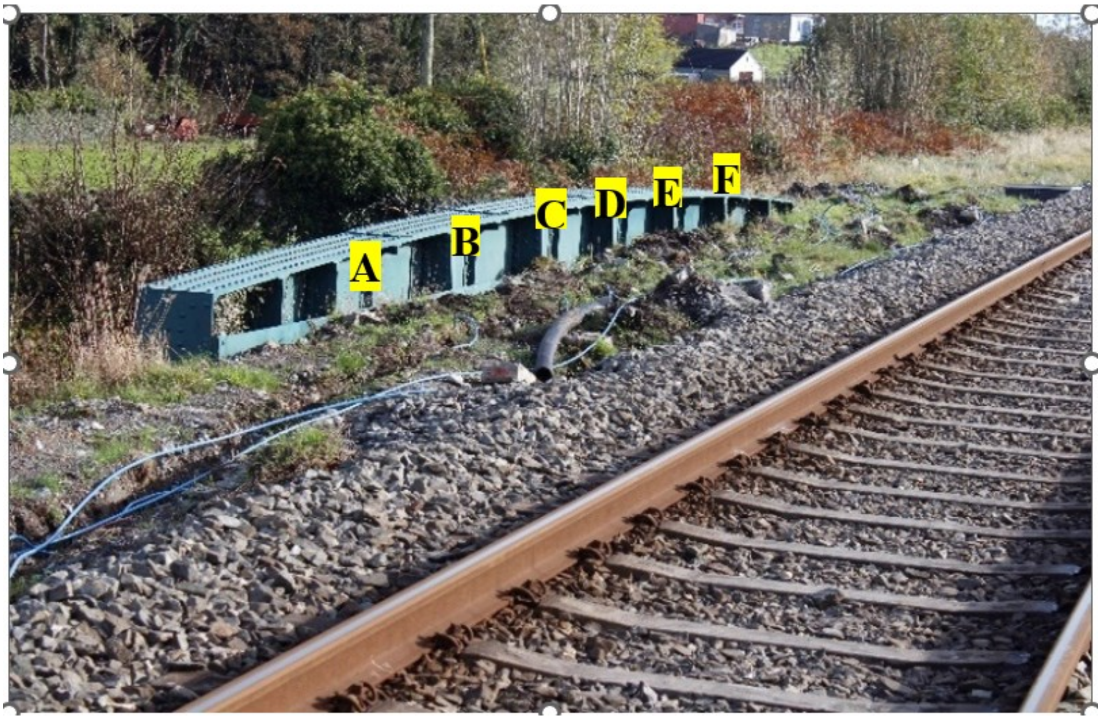

Figure 23. Instrumentation locations on the bridge

Testing was carried out in 5 stages, each involving sensors at two locations on the beam, while always keeping one location in common with the neighboring segment/stage. These correspond to A-B, B-C, C-D, D-E and E-F in Figure 23. The accelerometers were attached to the beam web at each location using magnetic mounting bases and accelerations were recorded at a scanning rate of 256 Hz. Recharging of the accelerometers was carried out after each phase using a car battery and DC inverter. It has been observed that in most of the measurements, the acceleration response damps out instantly after the train leaves the bridge, making it difficult to estimate mode shapes using only free vibrations. For that reason, the modal estimation is carried out using the forced accelerations, which provided reasonable excitation in the bridge. For each stage of measurement, the accelerations in response to 3 passing trains were recorded and transmitted wirelessly to a base station near the bridge. Recording was continued for two seconds of free vibrations after the passage of each train.

3.4 Experimental Validation of Concept

The first natural frequency of the bridge is calculated experimentally using a Fast Fourier Transform (FFT) from the forced and free vibration signals for each passing train (Table 3).

1st Natural Frequency								
Before rehabilitation					**After rehabilitation**			
Sensor Location.	Train.	Route	Forced Freq./ Hz	Free vibration freq. /Hz	Train.	Route	Forced Freq./ Hz	Free vibration freq. /Hz
A & B	1	Galway to Dublin	10.15	10.32	16	Galway to Dublin	9.66	9.64
	2	Limerick to Galway	9.72	10.26	17	Limerick to Galway	9.51	9.65
	3	Dublin to Galway	9.16	10.23	18	Galway to Dublin	8.98	9.65
B & C	4	Galway to Dublin	10.18	10.25	19	Dublin to Galway	7.20	7.39
	5	Dublin to Galway	10.10	10.27	20	Limerick to Galway	9.00	9.62
	6	Galway to Limerick	10.12	10.26	21	Dublin to Galway	9.29	9.62
C & D	7	Limerick to Galway	9.72	10.25	22	Galway to Limerick	9.59	9.65
	8	Dublin to Galway	10.54	10.33	23	Galway to Dublin	7.17	7.31
	9	Galway to Dublin	10.43	10.48	24	Limerick to Galway	9.84	9.66

D & E	10	Limerick to Galway	10.05	10.28	25	Dublin to Galway	7.31	7.65
	11	Dublin to Galway	10.04	10.10	26	Dublin to Galway	9.46	9.61
	12	Limerick to Galway	9.25	10.25	27	Limerick to Galway	9.37	9.65
E & F	13	Galway to Dublin	9.98	10.14	28	Galway to Dublin	9.49	9.57
	14	Galway to Limerick	9.03	10.01	29	Galway to Limerick	9.28	9.62
	15	Galway to Dublin	9.59	9.80	30	Galway to Dublin	7.24	7.38
Avg.			**9.85**	**10.22**	**Avg.**		**8.83**	**9.05**

Table 3. First bridge natural frequency from the bridge accelerations to each passing train at UBG165.

It can be seen from Table 3 that the average frequencies have decreased after the rehabilitation for both forced and the free vibrations. This change is consistent with a release of support stiffness due to the installation of new bearings. The frequency change for the numerical study is higher due to the idealised conditions. However, in reality the deviation obtained from experimentation is, although lower than the numerical model but is reasonably high and indicates that the stiffness change is approximately 10%, indicating that a definitive change in structural condition has occurred. Although this change indicates significant bridge damage, further mode shape analysis must be carried out to detect specific bridge bearing seizure.

The data from each stage of the field test is analysed using frequency domain decomposition (FDD) to obtain a segment of the first mode shape. For each stage, the mode shape segment is calculated three times, once for each of the passing trains. Over five stages, with three segments of mode shape per stage, there are (35=) 243 possible ways in which the segments can be combined. All 243 estimates of the mode shape are normalised and presented in Figure 24.

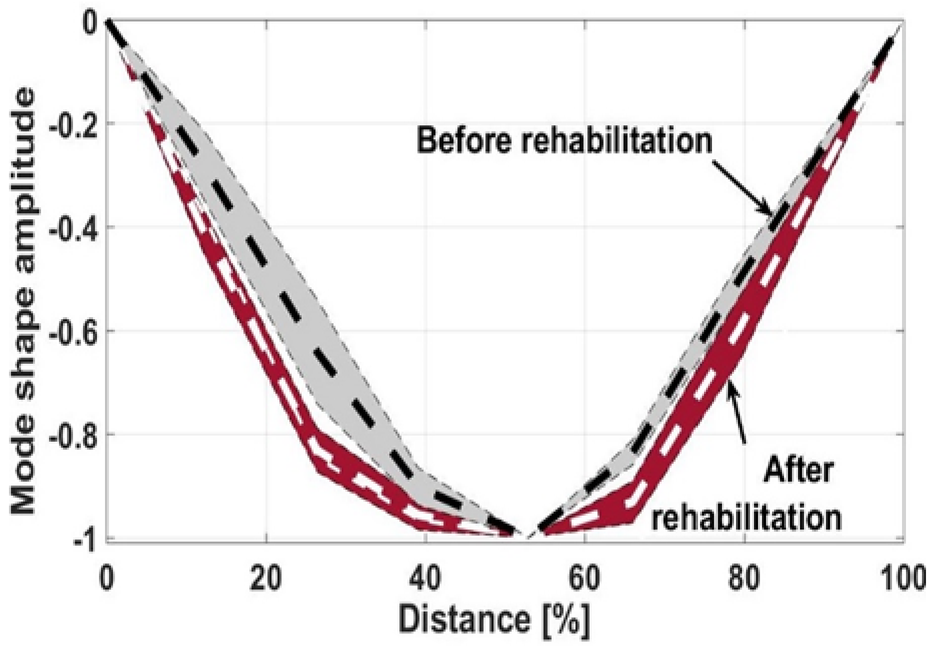

Figure 24. Mean ± one standard deviation of 1st bridge mode shape before and after the rehabilitation

for the pre- and post-rehabilitation measurements.

For details see: Khan, Muhammad Arslan, Daniel P. McCrum, Eugene J. OBrien, Cathal Bowe, David Hester, Patrick J. McGetrick, Connor O'Higgins, Miguel Casero, and Vikram Pakrashi. "Re-deployable sensors for modal estimates of bridges and detection of damage-induced changes in boundary conditions." *Structure and Infrastructure Engineering* 18, no. 8 (2022): 1177-1191.

4. Edge Solutions for Monitoring

4.1 Context

Directly implementable solutions at the edge, with demonstrated benchmarks are needed for the SHM sector to make a paradigm shift to an IoT based future, and to accommodate the lifetime monitoring demands, combined with new detection algorithms. To address this need, a low-cost, low-power SHM prototype using off the shelf components within an open source IoT framework was demonstrated.

4.2 Design of Solution

The low-power wireless sensor system consists of an edge device and a gateway. The edge device consists of sensors, a microcontroller, and a wireless LoRa transceiver. The gateway, situated within the range of the edge device, consists of a LoRa gateway receiver, a microprocessor and a Wi-Fi or cellular module to communicate data to a cloud platform.

The edge device continuously records data from three accelerometers. Due to the high sampling rate of the accelerometers and the transmission limits of low power wireless communication protocols, the data is first locally stored and processed before features are extracted and wirelessly transmitted in a batch via LoRa. The data, following acquisition, is stored, processed and subsequently transmitted as shown in Figure 25.

For data acquisition, data ready interrupt is used to sample voltage from the accelerometer at a set interval corresponding to a desired sampling frequency. Using the inbuilt timer in the microcontroller, the Analog to Digital Converter (ADC) is triggered at the pre-set sam-pling interval and the ADC reads the reference voltage (Vref) value for the analog pin con-nected to the sensor. Accelerometer, as a slave device, only records a voltage on command from the master device. Depending on the number of ADC in the microcontroller, for mul-tiple analog inputs, such as multiple sensors or multiple axis, the ADC must switch over each analog pin during the sampling interval. For data storage, a double buffering tech-nique is used to simultaneously sample incoming data and carry out signal processing and data transmission on already recorded data. The Direct Memory Access (DMA) con-troller is used to read the datapoint and store it in a buffer. Once the buffer is full, the data array is transferred for processing while a second empty buffer is being filled. For data pro-cessing, signal processing and feature extraction is carried out on the complete buffer and calculated features are sent to a First In First Out (FIFO) queue. Once sufficient values are stored in the queue, they are assembled into a data packet and encoded as ASCII data for the RF payload. Finally, for data transmission, the LoRa transceiver module is switched on from sleep mode and used to transmit the assembled data packet to the gateway, returning back to a sleep state once the transmission has been successful.

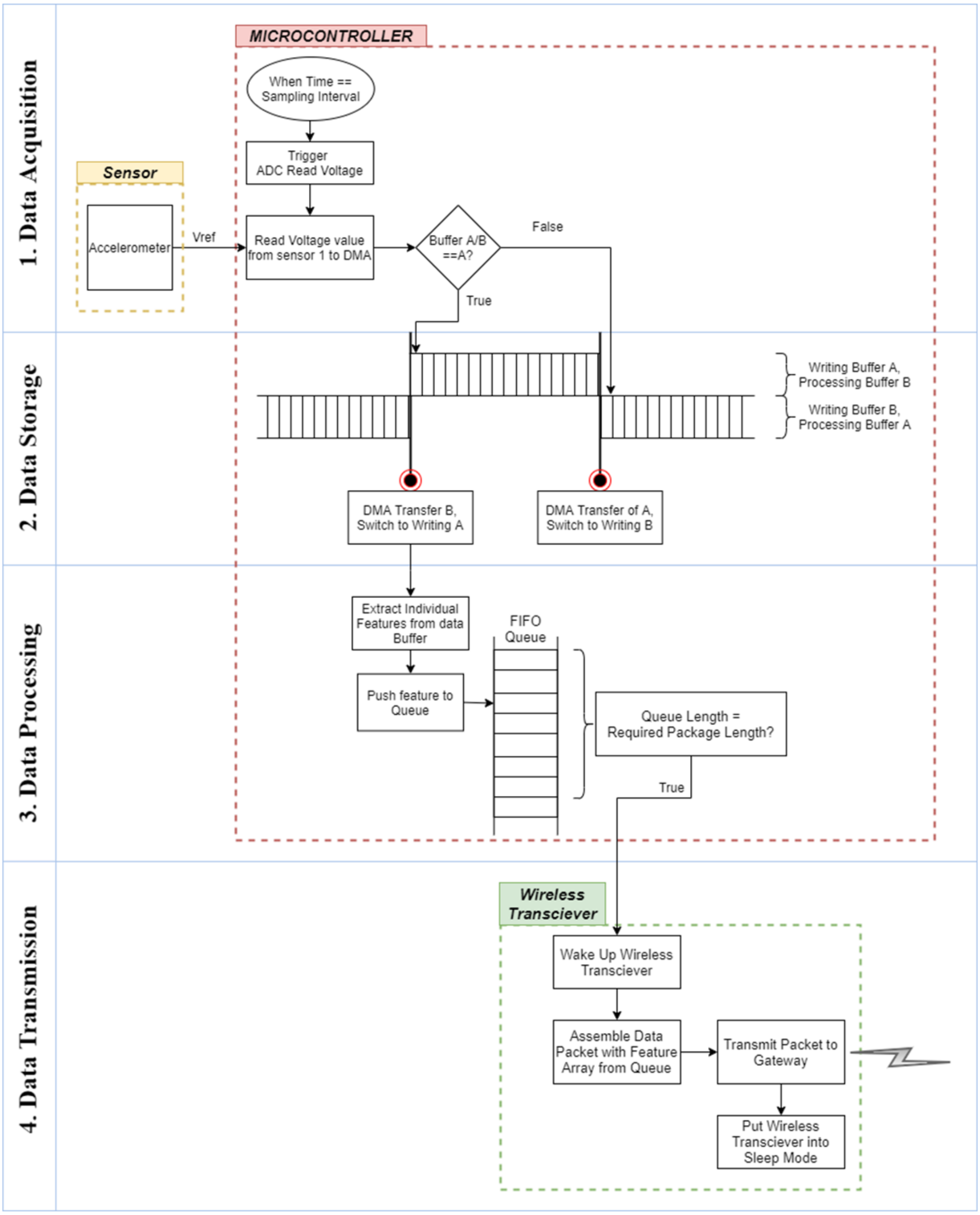

Figure 25. Data flow in edge solution design for monitoring

packet to the gateway, returning back to a sleep state once the transmission has been successful.

4.3 A LoRa Framework

LoRa is a noncellular radiofrequency carrier signal which encodes information using a chirp spread spectrum (CSS) modulation scheme, enabling data communication over a long range (typically 1km-4km in dense and up to 45km in low density areas) with low power and minimum throughput. It is also the hardware that supports the modulation technology, including the LoRa chips and gateways, and is the physical layer in a Low Power Wide Area Network (LPWAN) system. A private LoRa network can be deployed for single applications leading to the advantage of larger message capacity compared to a public LoRaWAN gateway due to exclusive bandwidth, complete control over the end-to-end data transmission, and the ability for bidirectional command and control functionality to the gateway and edge devices.

LoRaWAN is the media access control (MAC)-layer protocol communications which is built on the LoRa modulation technology and hardware. LoRaWAN network architecture is laid out in a star-of-stars topology with a central gateway and multiple edge nodes in the network. It is best suited for public wide area networks (WAN) as all the channels are tuned to the same frequencies and its primary advantage is that only the edge sensor needs to be deployed in a monitoring application. However, they are limited by fair usage and access policies. The installation of a private gateway is necessary when a LoRaWAN network is not available in the region of deployment

LoRa is linked to spread spectrum modulation where data can be spread in both frequency and time to increase the robustness and range of transmission by increasing the receiver's sensitivity. The range and throughput of data transmission depend on the physical bandwidth for radiofrequency modulation (BW), coding rate (CR) and spreading factor (SF).

Larger bandwidths allow for a higher effective data rate which reduces the transmission time but also reduces the sensitivity. The CR is for Forward Error Correction (FEC), which is combined with the spread spectrum technique to further increase the receiver sensitivity and correction. The SF affects the rate of data transmission, LoRa supports multiple spreading factors (between 7-12) to decide the tradeoff between range and data rate. A lower SF results in a higher data transmission rate but also a lower range of transmission due to the lowered immunity to interference. The data rate ranges from 300 bps to 37.5 kbps depending on spreading factor and channel bandwidth.

An uplink LoRa packet consists of a set of preamble symbols, an optional header, a variable-length payload field and an optional cyclic redundancy check (CRC) field. PL represents the number of payload bytes and header is composed of preloaded information. LoRa frame format can be either implicit or explicit where an explicit packet includes a short header containing information about the bytes, CRC and coding rate used in the frame.

The data rate (DR) is defined by SF and BW, so the maximum packet size roughly depends on the distance to the nearest gateway. As LoRa operates in the unlicensed scientific bands, the DR is also limited by the specification for each region. For the European 863-870 MHz band, the maximum application packet size varies from 51 bytes for slower DR to 222 bytes for faster rates. The Header is composed of preloaded information and DE indicates the absence (0) or presence (1) of the header in the packet.

The gateway or base station has a much higher communication capability, processing power and memory than the wireless sensor node and is situated in a location within the range of the edge devices where power supply is not an issue. The gateway receives and parses the LoRa data packets and transmits them onto a cloud data management platform. For LoRa, the gateway can be private (user implemented) or public (LoRaWAN). In this paper, a private LoRa gateway setup is implemented, which consists of a microprocessor, a wireless LoRa receiver and internet connection via a cellular or WiFi module. The LoRa gateway transceiver can receive data from multiple edge devices in a one-to-one star topology. The gateway is not a low power set up and needs to be connected to a mains power source. It is in a constant listening state for incoming data packets from the edge nodes. These data blocks are parsed and transmitted via Wifi or 4G to a cloud IoT management dashboard. Data can then be stored, analysed and displayed on a dashboard on any IoT management platform.

4.4 Instrumentation and Measurement

Figure 26 presents a typical instrumentation approach on a beam using the proposed solution. Data was collected in three different ways. First, an oscilloscope monitored each shaker input and recorded the raw acceleration data at 500 Hz. Secondly, each accelerometer was connected to the analog inputs of Arduino Due used for the experiments, where the values are printed via the USB serial port to a local PC. This method uses the Arduino Due as an oscilloscope. Finally, the LoRa setup described was used to extract root mean square (RMS) features from the raw data and transmit to a local PC via the LoRa gateway. Figure 27 summarises the data collection methods.

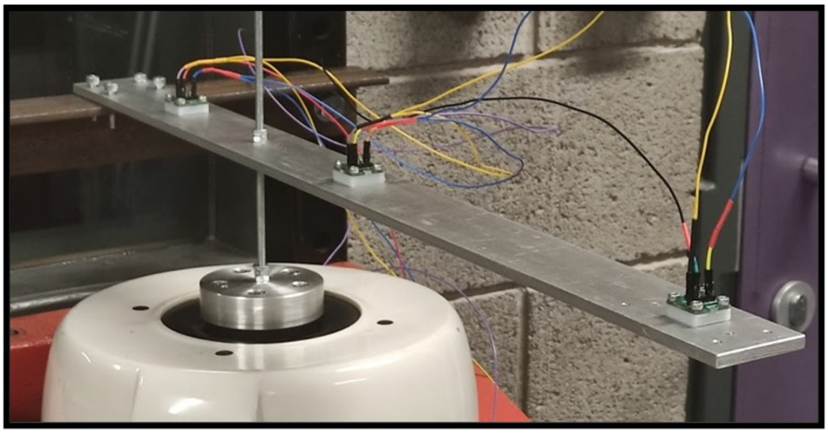

Figure 26. Data flow in edge solution design for monitoring

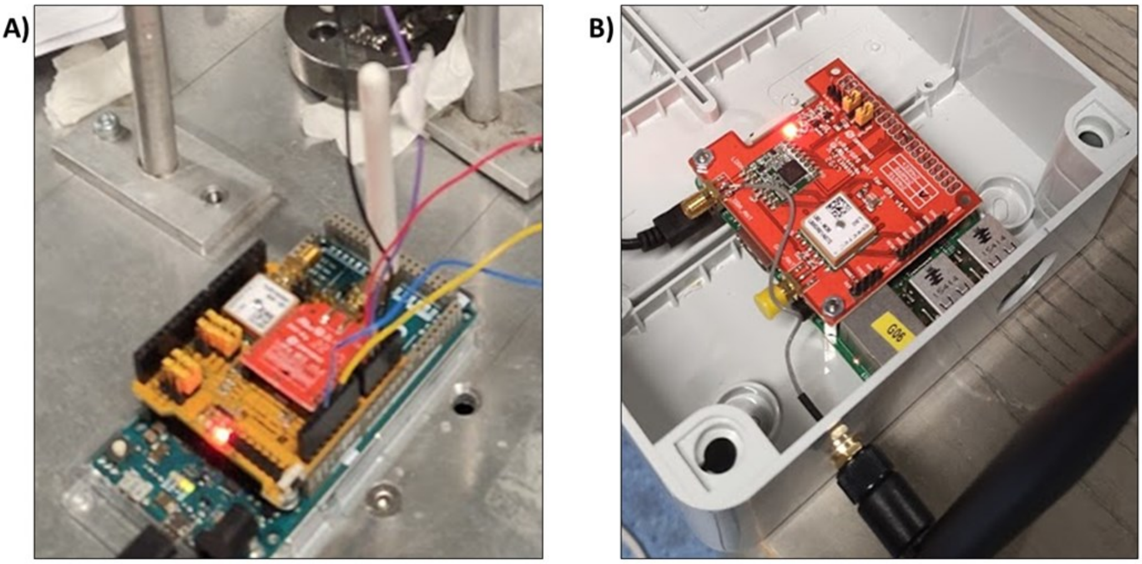

Figure 27. LoRa Transmission via A) Edge device, Arduino Microcontroller with LoRa shield B) Gateway, Raspberry Pi Microprocessor with LoRa receiver Hat.

4.5 A Low Power IoT Framework

Figure 28 shows the three sections in the IoT framework - the edge device, gateway and data management platform used in this paper. The LoRa transmission settings and gateway configuration in this application is based on the low-cost and low-power IoT framework developed in the H2020 EU WAZIUP project, also establishing repeatability and adaptability.

For the edge device setup, the Arduino Due microcontroller was used which has a single built-in ADC and Vref = 3.3 V. The Arduino samples the data from the accelerometers at 500 Hz. The Arduino Due is a 32bit CortexM3 ARM microcontroller with an 84MHz clock. A shield is attached to the microcontroller for LoRa communications.

A 3-axis, ±3g, ADXL335 micro-electromechanical systems analog accelerometer is used for data measurement. The evaluation board is used for the prototype to easily connect the accelerometer to the pins of the microcontroller (Raspberry PI 3). The accelerometer has a 350 µA power consumption and a 0.5 Hz-1600 Hz measurement range in the X and Y axes, and a 0.5 Hz-550 Hz range in the Z axis, respectively.

This value must be determined for each sensor before measurement is carried out. For the three accelerometers used in this experiment the sensitivity values were: 305 mV/g, 302mV/g and 299mV/g for accelerometers 1, 2 and 3 respectively.

Feature extraction at the edge is required due to limits on data packet sizes and this paper considers RMS value and the peak natural frequency as extracted features. For long term continuous monitoring, features need to be either calculated or averaged over time windows that can be transmitted in small packets over intervals of several minutes.

For the EU863-870 unlicensed bands, the maximum available payload size per LoRa message is 222 bytes for a datarate of 4-7 (BW 125, CR,5, SF 12). To obtain enough samples, features are calculated over 1-second of recording. Using the above configurations and a maximum payload of 222 bytes, a payload of 128 bytes for the data packet and is used.

An 8-bit ASCII encoding is considered and each feature is stored to flash memory (512 kB). Data is queued to be sent out at 3-minute intervals at a later time. In a full-scale scenario, the interval over which the features are calculated would be much longer.

The Arduino Due is a 3.3V microcontroller and has an estimated power consumption of 100mA. Overall 3 accelerometers are powered by the arduino and each have a current draw of 0.35mA.

The LoRa shield has a current draw of 20 to 120mA while transmitting (depending on the boosting for maximising range) and 0.2 micro amps while in sleep mode. That is an estimated range of 0.4W to 0.7W while the LoRa device is transmitting and 0.3W while the accelerometers are recording and the LoRa device is in sleep mode.

A field implementation of this prototype would require the development of an Application Specific Integrated Circuit (ASIC) with application specific code to replace the Arduino Due microcontroller, significantly reducing the power draw.

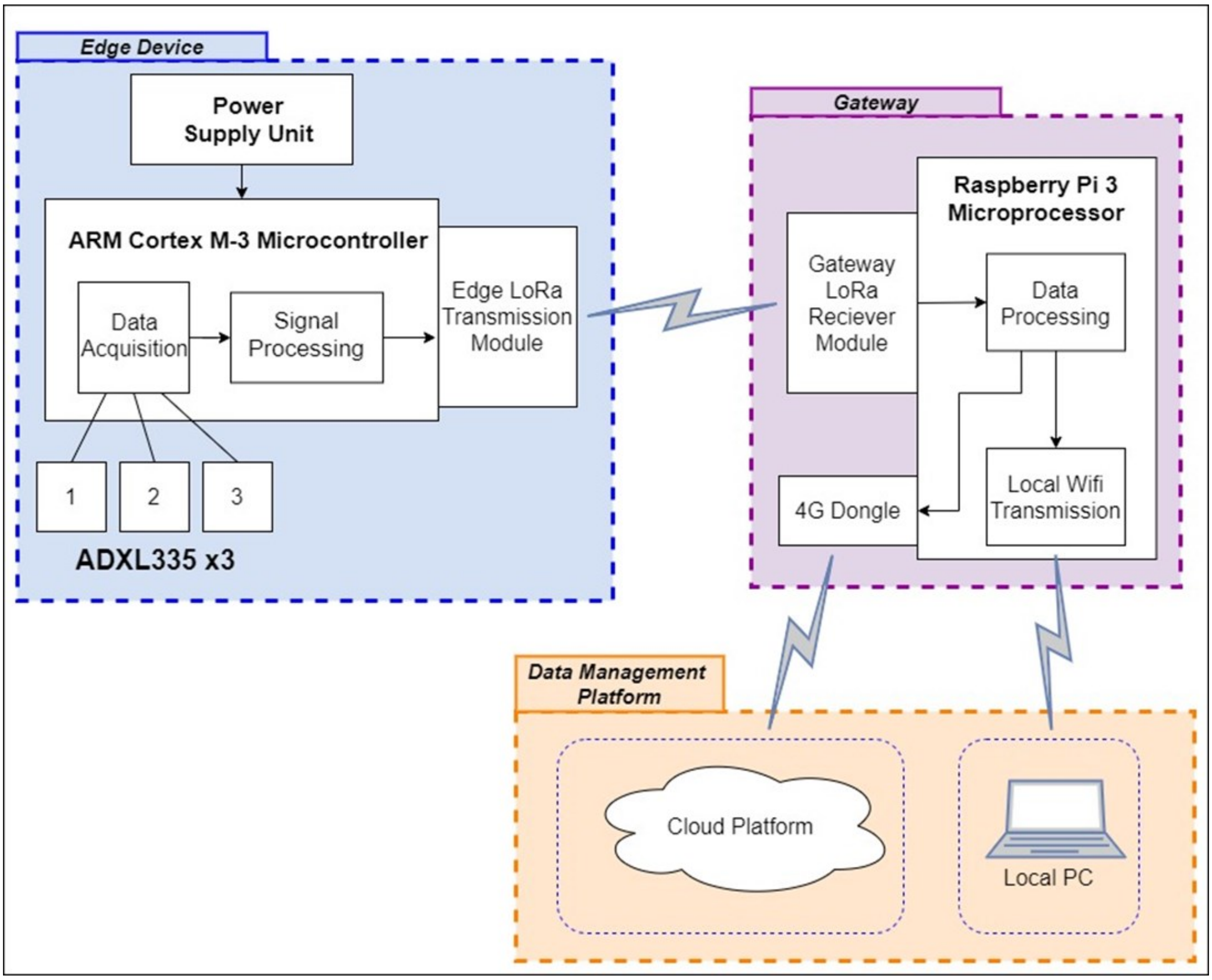

Figure 28. A low power SHM IoT framework

This framework can be used in future for a range of applications related to SIRMA infrastructure monitoring.

For details, see: Buckley, T., Ghosh, B., & Pakrashi, V. (2021). Edge structural health monitoring (E-SHM) using low-power wireless sensing. *Sensors*, *21*(20), 6760.

5. Instrumented Train as Sensor for Monitoring

5.1 Context

It has been shown in this report that dynamic response signatures of features of interest like damage and consequently there is a possibility of instrumenting trains to act as moving sensors across the network.This possibility is investigated jointly by UCD and Irish Rail, while also establishing national level collaborations. Ireland has a relatively small network (Figure 29) of train network but such state of the art solutions can be demonstrative for other countries and networks as well. The section is also demonstrative of the co-creation and evidence of the activities related to WP7.

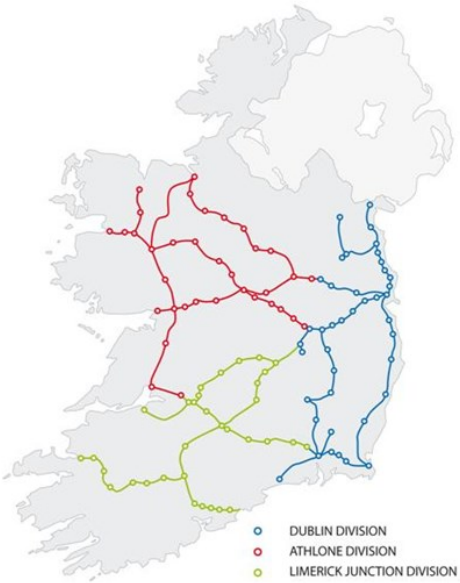

Figure 29. Train network of the Republic of Ireland.

5.2 Monitoring System and Bogie Instrumentation

Figure 30 presents locations of instrumentation and how a train can be converted to a moving sensor across the network. Figure 31 shows the top view while Figure 32 shows the side view.

Instrumented bogies with accelerometers typically relate to the instrumentation aspects, along with GPS - but the results are limited to the uncertainties and calibrations of the sensors. Even though the needs of the monitoring features require low acceleration levels, the movement of trains lead to shocks and the accelerometers must be robust against shocks and also exposure to harsh weather conditions.

This monitoring scheme was followed for Irish Rail in SIRMA in terms of development of the measurement chain by combining small individual off the shelf components. Anemometers can also be connected to the front and the back of the train, but with geometric constraints around how much extension is allowed around the train in space.

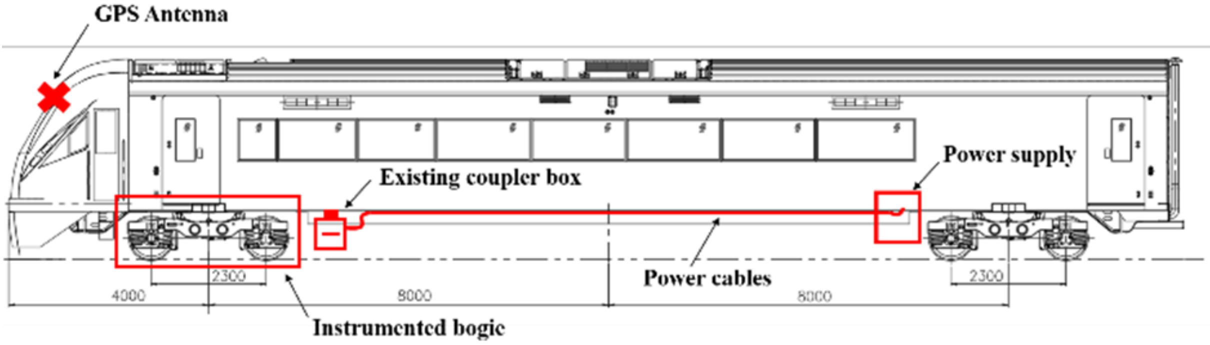

Figure 30. Sensor placement ideas for converting a train to a moving sensor for monitoring infrastructure

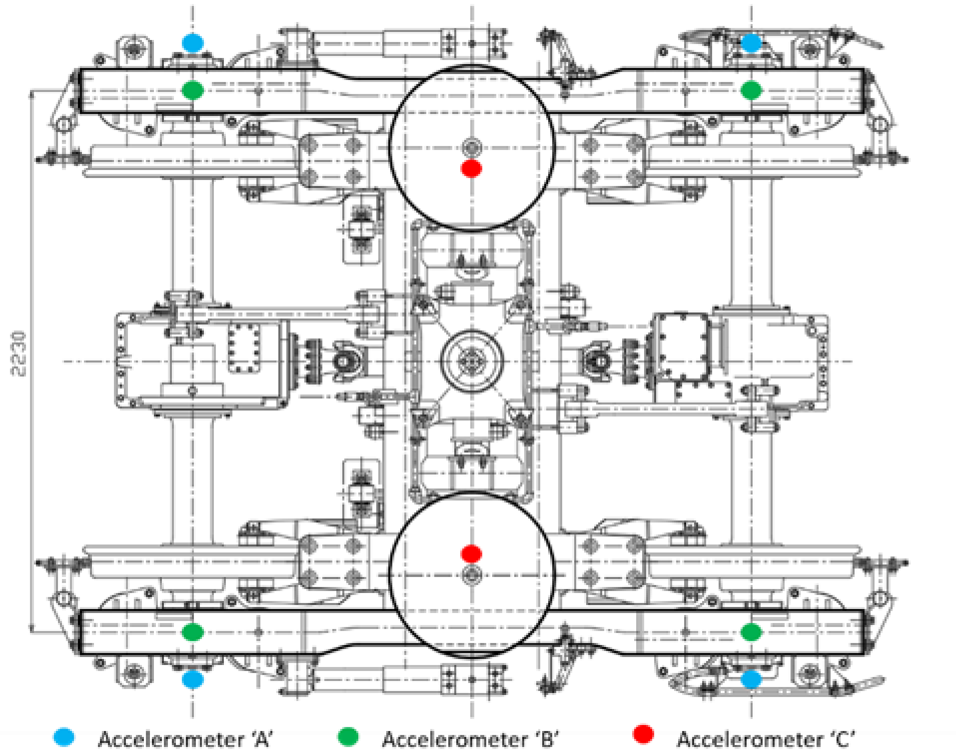

Figure 31. Acceleration placement ideas for converting a train to a moving sensor: top view

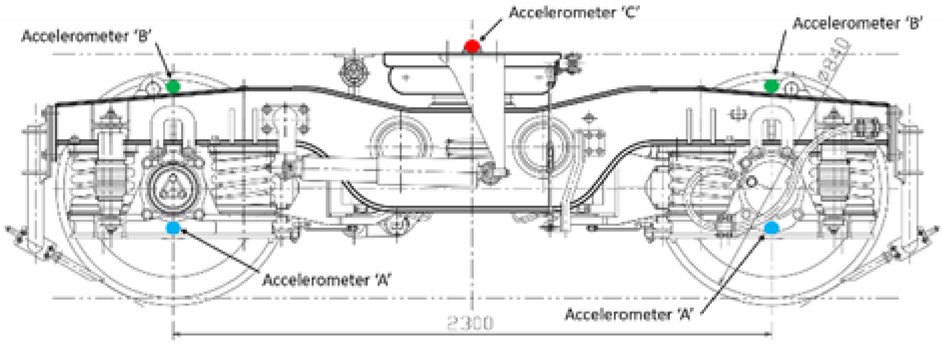

Figure 32. Sensor placement ideas for converting a train to a moving sensor: side view

A Hyundai-Rotem InterCity fleet car was considered for instrumentation which can be carried out during Regular Train Servicing. The GPS antenna should be installed on a flat surface in the head unit in the cab, facing the sky (satellites). The sensors are to be fixed at various location on the trailer bogie of the leading car as 'Instrumented bogie'. The communication and data transmission from sensors to the data logger is ensured through cables routed alongside existing cables. Data logger is fixed in the existing disused emergency coupler box located to the rear of the instrumented bogie. This location for the data logger ensures the access to the data every 5 weeks or so when the regular train servicing is scheduled, but not restricting it to it.

Leading bogie of the leading car was chosen to be instrumented with 10 accelerometers in total. Three types of accelerometers are considered for this.

5.3 Measurement System Organisation

Sensors should be selected to measure vibration in a hostile and noisy environment. DAQ hardware and software were designed for the type of signal to be measured, signal frequency sampled, error level enabled.

Figure 33 presents the system's architecture and Table 4 presents the details of typical sensors. There are three axis in the coordinate system that should be considered when designing the system: X-axis runs along the rail, Y-axis is transversal to the rail and Z-axis is vertical, as defined in EN 13848.

A modular data logger capable of recording a minimum of 20 channels has been chosen. The system was configured to start out recording 30 s before the motion is detected. When the system detects no motion for 5 minutes, it ends the recording. For every recording session, a new data file is generated.

The system was programmed to switch off and turn on again when the train is operated according to the power on the train.

A better communication between the GPS antenna and the satellites is ensured choosing the available location next to 'Direction Indicator' in the cab. The GPS system has an accuracy of ± 1 m horizontal and ± 2 m vertical.

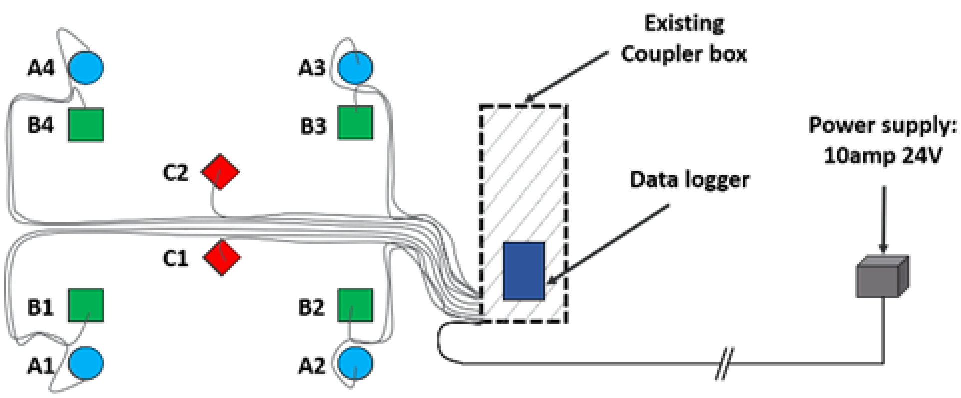

Figure 33. System design and measurement architecture

Sensor Name	Property	No. Sensing Axles	Range	Sampling Frequency	Resolution	Shock	Sensor noise	Temp. range	Ingress Protection
A1	Unsprung mass	Tri-axial	±50 g	Variable - Normal operation: 500 Hz	12 bit (min)	200 g	<1%	-40 °C ÷ +80 °C	IP 64
A2		Uni-axial							
A3									
A4									
B1	Sprung mass	Tri-axial	±10 g						
B2		Uni-axial							
B3									
B4									
C1	Sprung mass	Tri-axial	±10 g						
C2		Uni-axial							

Table 4. Sensor specification for measurement design

5.4 Measurement Possibilities

The proposed system can measure and monitor several aspects and some of it has been investigated as a pilot as a part of implementation of WP7, working closely with the WP5 benchmark. For details, Deliverable 5.2 on numerical and experimental repository should be consulted.

Track settlement (Figure 34), rail degradation (Figure 35), scour detection (Figure 36) and bridge strike (Figure 37) are some of which can be investigated. With anemometers, stability against wind can also be assessed.

The outcomes can also impact temporary speed restrictions, wind effect, weheel wear and bearing health (Figure 38).

Figure 34. Track settlement can be assessed by train-track interaction monitoring by train as a moving sensor

Figure 35. Rail wear can be assessed by train-track interaction monitoring by train as a moving sensor

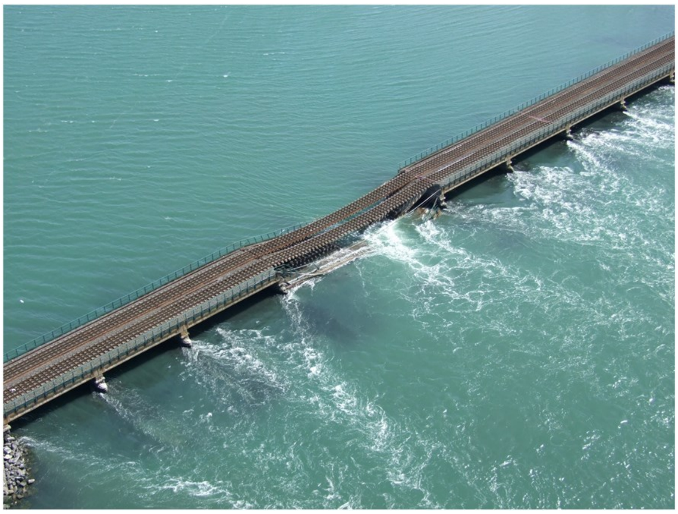

Figure 36. Scour impacts can be assessed by train-track interaction monitoring by train as a moving sensor

Figure 37. Track settlement can be assessed by train-track interaction monitoring by train as a moving sensor

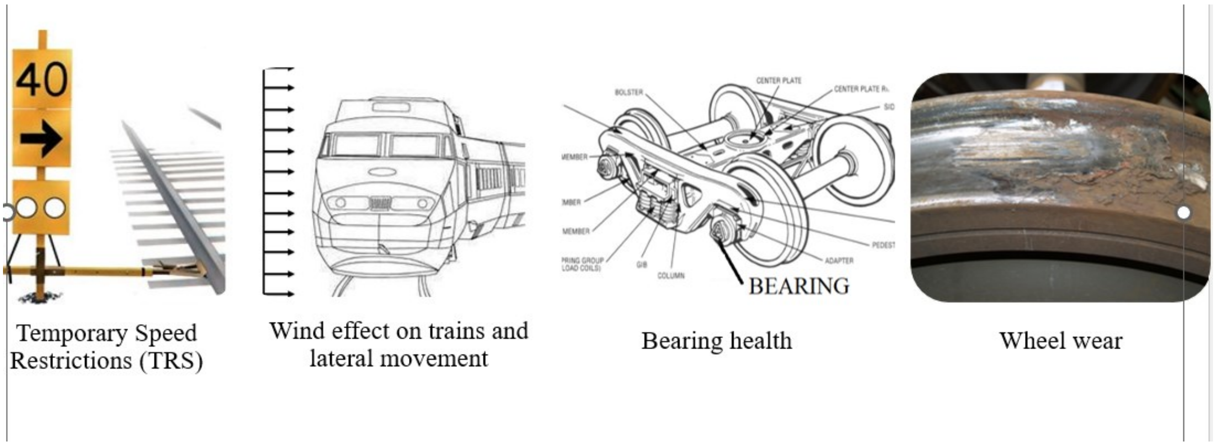

Figure 38. Impacts of monitoring by using train as a moving sensor

For details, see: Micu EA, OBrien E, Bowe C, Okosun FO, Morgan D and Pakrashi V. (2021). Instrumenting an Operational Train for Continuous Monitoring of Bridges and Track. Eurostruct 2021 – 1st Conference of the European Association on Quality Control of Bridges and Structures – Eurostruct, Padova, Italy

5.5 Comments on Deployment of Sensors

The project was impacted by Covid19 situation for a long time and only after a PAF revision was it possible to place order for the equipment. However, several Irish Rail real bridge data and instrumentation were carried out and the co-creation thrived despite Covid19 challenges.

Furthermore, this project also investigated some new sensors and it was observed that energy harvesting based monitoring of infrastructure (Demartino et al., 2022) can be particularly promising in future.

Acknowledgements

This report was carried out in the framework of the Strengthening the Territory's Resilience to Risks of Natural, Climate and Human Origin (SIRMA) project, which is co-financed by the European Regional Development Fund (ERDF) through INTERREG Atlantic Area Programme with application code: EAPA_826/2018.

The sole responsibility for the content of this publication lies with the authors. It does not necessarily reflect the opinion of the European Union. Neither the INTERREG Europe programme authorities are responsible for any use that may be made of the information contained therein.

References

Huseynov, F., Hester, D., Obrien, E. J., McGeown, C., Kim, C. W., Chang, K., & Pakrashi, V. (2022). Monitoring the Condition of Narrow Bridges Using Data from Rotation-Based and Strain-Based Bridge Weigh-in-Motion Systems. *Journal of Bridge Engineering*, *27*(7), 04022050.

Khan, Muhammad Arslan, Daniel P. McCrum, Eugene J. OBrien, Cathal Bowe, David Hester, Patrick J. McGetrick, Connor O'Higgins, Miguel Casero, and Vikram Pakrashi. "Re-deployable sensors for modal estimates of bridges and detection of damage-induced changes in boundary conditions." *Structure and Infrastructure Engineering* 18, no. 8 (2022): 1177-1191.

Buckley, T., Ghosh, B., & Pakrashi, V. (2021). Edge structural health monitoring (E-SHM) using low-power wireless sensing. *Sensors*, *21*(20), 6760.

Micu EA, OBrien E, Bowe C, Okosun FO, Morgan D and Pakrashi V. (2021). Instrumenting an Operational Train for Continuous Monitoring of Bridges and Track. Eurostruct 2021 – 1st Conference of the European Association on Quality Control of Bridges and Structures – Eurostruct, Padova, Italy

Demartino, C., Quaranta, G., Maruccio, C., & Pakrashi, V. (2022). Feasibility of energy harvesting from vertical pedestrian-induced vibrations of footbridges for smart monitoring applications. *Computer-Aided Civil and Infrastructure Engineering*, *37*(8), 1044-1065.

McGeown, C., F. Huseynov, D. Hester, P. McGetrick, E. J. Obrien, and V. Pakrashi. "Using measured rotation on a beam to detect changes in its structural condition." *Journal of Structural Integrity and Maintenance* 6, no. 3 (2021): 159-166.